NASA Technical Memorandum 79247

NASCAP MODELLING OF ENVIRONMENTAL-CHARGING-INDUCED DISCHARGES IN SATELLITES

N. John Stevens and James C. Roche
Lewis Research Center
Cleveland, Ohio

Prepared for the
Annual Conference on Nuclear and Space Radiation Effects
sponsored by the Institute of Electrical and Electronics Engineers
Santa Cruz, California, July 17-20, 1979

NASCAP MODELLING OF ENVIRONMENTAL-CHARGING-INDUCED DISCHARGES IN SATELLITES

by N. John Stevens and James C. Roche

National Aeronautics and Space Administration
Lewis Research Center
Cleveland, Ohio 44135

SUMMARY

A study of the charging and discharging characteristics of a typical geosynchronous satellite experiencing time-varying geomagnetic substorms, in sunlight, is conducted. The NASA Charging Analyzer Program (NASCAP) is used. An electric field criteria of 1.5×10^5 volts/cm to initiate discharges and transfer of 67% of the stored charge is used in this study, based on ground test results. The substorm characteristics are arbitrarily chosen to evaluate effects of electron temperature and particle density (which is equivalent to current density). It has been found that while there is a minimum electron temperature for discharges to occur, the rate of discharges is dependent on particle density and duration times of the encounter. Hence, it is important to define the temporal variations in the substorm environments.

INTRODUCTION

Since the late 60's, geosynchronous satellites have been experiencing encounters with geomagnetic substorms-plasma clouds in the magnetosphere.[1] These clouds charge spacecraft exterior surfaces to negative voltages as large as -19 kV during eclipses[2] and -2 kV in sunlight charging encounters.[3] This phenomenon of substorms charging satellites is called "spacecraft charging."[4] As a result of this charging, electronic switching anomalies, logic upsets and thermal control coating degradation have been observed.[5]

For the past 4 years spacecraft charging phenomena have been the subject of a coordinated AF/NASA investigation.[6] The objective of this investigation is to devise design guideline and test standard documents to aid engineers in building spacecraft that will be immune to spacecraft charging anomalies. This objective is to be met by a combined ground technology and space flight program aimed at defining the substorm environment, evaluating insulator response in ground tests, developing analytical tools to describe charging and discharging, modifying materials to minimize charging and finally, validating ground technology against actual space flight data obtained from the P78-2, SCATHA satellite.

While this investigation is still underway, there are sufficient results to conduct an initial study of the response of a typical, simplified geosynchronous satellite to idealized geomagnetic substorms. Such analyses have been conducted in the past using steady-state results from lumped parameter, equivalent circuit techniques.[8,9] However, studies of the charging of insulators surfaces in space-type environments have indicated that it takes hours for the insulators to reach equilibrium surface voltages.[10] While substorms can last up to 8 hours, they are transient in intensity and plasma density.[8] Hence, transient com-

puter simulations should be used to determine the response of the surfaces to substorms. The NASA Charging Analyzer Program (NASCAP) can compute this transient charging behavior and even allow discharges to occur.

The purpose of this paper, then, is to evaluate the charging of a geosynchronous satellite in both sunlight and time-varying substorm conditions, so that conditions in which discharges occur can be determined. A discharge criteria based on the ground simulation tests is used. The NASCAP model, the discharge criteria and geomagnetic substorms and the results are presented in the following sections.

NASCAP MODEL OF GEOSYNCHRONOUS SATELLITE

NASCAP Description

The NASA Charging Analyzer Program (NASCAP) has been described previously in the literature[11-13] and is only briefly summarized here. NASCAP is a quasi-static computational code; that is, it assumes that the current balance is a function of environmental parameters, electrostatic potential, magnetostatic fields and material properties at each instant of time. It is capable of analyzing the charging of three-dimensional, complex bodies as a function of time for given space environmental conditions. It includes consideration of dielectric material properties (e.g., secondary emission, backscatter, photoemission, and bulk and surface conduction) and computes currents involving these materials in determining the potential distributions around the body.

The body must be defined in terms of rectangular parallelipipeds, sections of parallelipipeds or flat plates within a 17 by 17 by 33 point grid. Seven separate conductors can be specified with the first conductor capable of floating with respect to space while the others can be biased with respect to the first. The environment can be defined in terms of a single or double Maxwellian distribution[14] by specifying particle temperatures (in electron volts) and number densities. Environments corresponding to both quiescent conditions and to severe substorms can be specified. The code outputs a variety of graphic displays showing the model used, the voltage distributions for given environments at specified times, and particle trajectories (if desired).

Satellite Description

The satellite model chosen for this evaluation is shown in figure 1. It is representative of a 3-axis stablized, geosynchronous, communications satellite. It consists of two, large solar array wings and a central spacecraft body. The overall dimensions are 9 m across the solar array wings, by 2.4 m across the spacecraft. Each square in the NASCAP model is 0.3 m by 0.3 m.

The solar array wings are each 3 m by 1.8 m. They are modelled as thin, flat plates with 0.015 cm (6 mil) silica cover slides on the sun facing side and 0.010 cm (4 mil) Kapton substrate. This represents a flexible substrate solar array system capable of producing a total power output of about 1 kilowatt. This system is assumed to be operating such that one wing is at +25 volts with respect to the spacecraft body while the other is at -25 volts. Aluminum

patches on the wings are the NASCAP simulation of the metallic interconnects in the array. The code cannot simulate small gaps, so these are lumped together as shown. These metallic areas represent 10% of the solar array area which is a good approximation to a typical solar array.

The spacecraft body is modelled as an octagon 1.8 m by 1.5 m deep. On the Earth facing side are two antennas modelled as octagons 0.9 m by 0.3 m high. On the opposite end is an apogee insertion motor (AIM) modelled as an octagon 1.2 m by 0.6 m deep. The materials used on this body are limited to 0.010 cm (4 mil) FEP Teflon on the Earth facing and rear sides, 0.010 cm (4 mil) Kapton on the apogee insertion motor sides and antenna covers, 0.015 cm (6 mil) silica as the Optical Solar Reflector (OSR) radiator coatings, and aluminum as representative of all exposed metal surfaces.

NASCAP Discharge Simulation

The present version of the NASCAP code contains the capability of simulating discharges in materials.[13] This simulation consists of a charging interruption when the differential voltage between the insulator surface and the conductor underneath exceeds a specified voltage. When this limit is exceeded charge is transferred from the insulator to the conductor underneath (depth of discharge also specified by user) and the charging simulation continues.

This discharge simulation is a first approximation to actual discharges. It is known that discharge processes involve depletion of charge over large areas[15] which implies a coupling mechanism (which is not included in NASCAP) and involves loss of charge to space.[16-17] However, even with the present limitations this study of satellite behavior does indicate those areas where discharges can occur and does show the repetition of the charge-discharge cycle.

From the laboratory test results it is known that discharges are initiated at edges, gaps, seams or imperfections in insulator surfaces.[18] The discharge threshold voltages for insulators commonly used on satellites have been measure..[19] For this simulation the criteria for discharge is based on this edge voltage breakdown concept and the breakdown voltages determined in the laboratory testing. For the Teflon and Kapton surfaces breakdowns are assumed to occur when the electric fields exceed 1.5×10^{-5} volts/cm and for the silica when the electric field exceeds 5×10^{4} volts/cm (since it discharges at a lower value than Teflon). The 67% transfer of charge that occurs in a discharge is based on experimental investigations.[15]

GEOMAGNETIC SUBSTORM ENVIRONMENT

The available information on the geomagnetic substorm environment is based primarily on data from the ATS-5 and -6 Auroral Particles Experiments.[1-4,8] A study of these data indicates a number of factors which must be considered in any evaluation of spacecraft performance. First, particle energies and current densities are not constant over the substorm period. This is illustrated by the January 2, 1970 substorm shown in figure 2. Second, there is a large variation in substorm duration and intensity (as indicated by the variation in the charging measurements on ATS-5 and -6). Third, the electron current density is low

when the average electron temperature is high. Conversely, the electron current density is high when the average temperature is low. Finally, the relationship between the electron and proton average energies and current densities is relatively linear with the proton energies being twice the electron and the proton current density 1/50 the electron.

Since there is this variation in particle parameters in substorms, it was decided to determine the effect of particle number densities on spacecraft potentials before establishing the substorm environments to be used in the study. This was accomplished by using a substorm with electron temperature of 8 keV, proton temperature of 14 keV and plasma densities of 0.2, 0.5, and 1 particle per cubic centimeter. The spacecraft model was used with sunlight coming in at a 27° angle to the array normal (June simulation). The simulation was run on the computer for a 2400 sec time period in 120 sec steps. The results are shown in figure 3. As shown the particle density has a significant effect on the spacecraft surface potentials and therefore, must be considered as a parameter in determining the spacecraft response to substorms.

Hence, for this study, three categories of substorms are defined (see fig. 4). Category 1 has a mild intensity with an electron temperature of 5.6 keV, proton temperature of 14 keV and plasma densities of 0.2 cm^{-3} in the first or low density case and 0.6 cm^{-3} in the high density case. This environment lasts for 2400 seconds for low density runs, 800 seconds in a cold plasma (1 eV temperatures for both electrons and protons and 5 cm^{-3} plasma densities), 2400 seconds at the high density, followed by 700 seconds in the cold plasma again. Category 2 environment is arranged in 30 minute steps at 8, 4, 6, and 3 keV electron temperatures. This could simulate a double peaked variable substorm as shown by the dashed line in the figure. Proton temperatures are all twice the electron temperatures. A low density and high density case are also used in this category. Category 3 environment is a single peak substorm simulated by 30 minute steps at 12, 8, and 4 keV electron temperatures with proton temperatures at twice these values. Plasma densities are defined for both a low and high density case.

For all environments sunlight is assumed to be fixed at the 27° incidence to the solar array. All computations are made at a 100 second time interval.

COMPUTATIONAL RESULTS

Category 1 Substorm

In this phase of the analysis, the satellite is exposed to a substorm of moderate intensity (5.6 keV electron temperature and 14 keV proton temperature) and low particle density (0.2 cm^{-3}) for 40 minutes, then exposed to a cold plasma for 15 minutes, exposed to the same intensity substorm but with 3 times the particle density (0.6 cm^{-3}) for 40 minutes and then re-exposed to the cold plasma (see fig. 4 for substorm profiles). The purposes of these computations are first, to compare the predicted response of the satellite ground potential to the ATS-6 measured potential in the same intensity and particle density as the first substorm and second, to evaluate the effects of increasing the density.

The time history of the satellite ground and voltage of a typical shaded Teflon surface on the thruster side of the spacecraft is shown in figure 5(a). The predicted behavior of the solar array wing is shown in figure 5(b) for typical silica cover glass, interconnects and Kapton substrate. The predicted voltage distributions around the satellite for the 2400 sec (40 min) and 5600 sec (93 min) times are shown in figures 6(a) and (b). These voltage profiles show that the most severely charged surfaces exists in the Teflon and Kapton areas on the thruster end of the spacecraft, the Kapton substrate on the solar array and to a lesser degree, the shaded OSR radiator plate. Since the OSR's and the Kapton surfaces seem to follow the Teflon surface voltage trends, the data presentation will be limited to those shown in figures 5(a) and (b).

At the 2400 sec time of exposure, the spacecraft ground potential is predicted to be -715 volts. The ATS-6 ground potential measured for a substorm with the same characteristics is -700 volts. Hence, it appears that the NASCAP code can predict reasonable voltage values for sunlit substorm conditions.

These computations indicated that differential charging was not severe in the low density case. The shaded Teflon charged to about -1450 volts or only 735 volts more negative than the sunlit spacecraft ground. The solar array interconnects were held to be $\pm$25 volt with respect to the spacecraft ground (due to the imposed voltage bias). The silica cover glass was about 100 volts less negative than the interconnects while the Kapton substrate was about 500 volts more negative. At these differential voltages, no discharges were expected and none observed.

The exposure to the cold plasma (1 eV and 5 cm^{-3}) brought all potentials rapidly back towards zero volts. The insulator surfaces responded to the change in the environment sooner than the ground potential. During this transient condition, differential charging was reduced.

The second phase of this substorm caused the spacecraft ground to be driven to -1700 volts in the 40 minute substorm encounter. The higher particle density also makes the spacecraft differential charging more severe. The shaded Teflon charged to about -3100 volts or to a 1400 volt differential. This is close to breakdown according to the criteria used. If the substorm encounter were longer or the particle density slightly higher, then discharges would have occurred. On the solar array the differential voltages were also larger. The coverslide voltage was about 250 volts more positive than the interconnects while the Kapton substrate was about 1000 volts more negative.

The limitation of the differential charging observed in these calculations appears to be due to the limitation of photoemission from the sunlit surfaces. It has been observed that, in three-dimensional analysis of charging of objects in sunlight, that the voltage fields from the shaded insulators can expand around the object and cause the existence of a saddle-point which limits photoemission.[20] This effect seems to exist here and since the ground potential predicted agrees with the ATS-6 data, it appears to be real.

Category 2 Substorm

In this part of analysis, the satellite is exposed to a substorm that reaches two peaks of intensity; the first at a 8 keV electron temperature and the second at 6 keV electron temperature. The proton temperature is alway twice the electron. The purpose of studying this type of encounter is to determine the effect of precharging satellite surfaces prior to the second substorm peak. Two different particle densities were used in this evaluation to determine rate effects (see fig. 4 for substorm characteristics).

The time history of the spacecraft ground potential, shaded Teflon surface voltage and solar array voltages for both particle densities are shown in figures 7(a) and (b).

Low density case. - The spacecraft ground charges to about -1800 volts during the 8 keV electron temperature step in the substorm, continues to charge negative for about another 5 minutes after the substorm intensity relaxes to 4 keV electron temperatures. During the second peak intensity (6 keV electron temperature), the spacecraft ground is driven to about -2500 volts. When the substorm intensity again is reduced, the ground potential falls off to about -1200 volts. After the 3 keV encounter, it is assumed that the satellite moves into a cold plasma environment and is neutralized.

The shaded Teflon surface, charges up rapidly in the first substorm peak and between 900 and 1000 second, the differential voltage exceeds the breakdown criteria and a discharge occurs. After the discharge transferred the required amount of charge to the conductor beneath (and subsequently reduced the surface voltage), the charging of this surface began again at a slightly higher rate than previously experienced. The Teflon surface responds more rapidly to the environment change than the spacecraft ground. The surface remains negatively charged during the 4 keV phase of the substorm and responds rapidly to the next increase in electron temperature (to 6 keV). Differential charging builds up rapidly again so that a discharge occurs between 400 and 500 seconds after the transition to the second peak. A second discharge occurs 1200 seconds after the first. The characteristic behavior of these discharges are very similar to those observed in the laboratory experiments on discharges in Teflon.[19]

Discharges also occurred in the Kapton thruster surface and in the shaded OSR radiator panel, but at slightly different times. It is interesting to note that with these discharges transferring charge to the spacecraft, there is no apparent change in the spacecraft ground charging rate.

The solar array behavior is mild compared to the spacecraft body. The array simply charges in response to the environment. The silica cover slides are always positive with respect to the interconnects and while differential charging builds up in the substrate, it does not exceed the breakdown criteria.

High density case. - This case is far more interesting to observe since there is considerable discharging both in isolated cells on the satellite and in large areas of the satellite. As shown in the time histories (fig. 7), discharges started occurring (between 400 and 500 sec and between 800 and 900 sec)

during the first peak intensity encounter in the Teflon cells. Discharges also occurred in the shaded OSR's after 600 and 800 seconds. Again these discharges did not change the apparent charging rate of the spacecraft ground and the solar array. After the 1000 second computation a major discharge occurred which involved about 100 shaded surface cells around the satellite (including the Kapton surfaces of the solar arrays). Since the discharge simulation transfers charge from the insulator surface to the conductor beneath, a major discharge causes the spacecraft charge to be larger than before and results in the negative voltage spike which makes this type of discharge stand out. At this point in time the shaded Teflon and OSR's that had been discharging prior to this, did not discharge until after the major discharge. When the substorm intensity dropped to the intermediate level, the discharges stopped.

The above characteristics can be observed from the voltage profiles around the edge view of the satellite at various times through this sequence (see figs. 8(a) to (d)). At the 800 second point the spacecraft ground is charged to about -1250 volts and the voltage distribution around the satellite are as shown in figure 8(a). Between the 800 and 900 second computations discharges occur in the shaded Teflon and OSR's causing a collapse of the voltage profiles in those regions and subsequent recharging (as noted by the arrow on fig. 8(b)). The spacecraft ground is now about -1500 volts. Between the 1000 and 1100 second computations the major discharge occurred which drove the ground potential to -2400 volts and caused the voltage distributions shown in figure 8(c). Note that there are still strong voltage gradients in the thruster region. Between the 1200 and 1300 second computations the thruster region discharged causing the redistribution of voltage profiles shown in figure 8(d). Thereafter, the voltage profiles continued to respond to the satellite conditions.

As mentioned before, when the substorm subsided to the intermediate 4 keV electron temperature condition, all discharge activity ceased. In the second peak intensity, with its correspondingly high particle density (5 cm^{-3}), discharge activity returned within 200 seconds. Within the 1800 second duration of this second peak intensity phase of the substorm, there were four major discharges on the satellite and four separate occurrences of discharges in the shaded thruster region. Hence, it appears that a double peaked substorm will produce significant discharge activity especially if the particle densities are relatively high.

When the substorm subsided to the 3 keV electron temperature level, discharge activity again subsided and the surface voltages were slowly reduced as shown.

The discharge characteristics observed here again are similar to those seen in laboratory experiments: the rate of discharges seems to be more dependent upon the incident current density than to the electron temperature.[21] When the spacecraft ground potential becomes much more negative (when the major discharges occur), then the Teflon surface voltage also is driven more negative as observed in studies on charging rates.[22]

Category 3 Substorm

The final category of substorm used in this study is a single peak, severe substorm that rapidly rises to a very high electron temperature and slowly falls off to quiescent conditions. Two particle density profiles that differ by a factor of two are used (see fig. 4(c)). The purpose in studying this type of substorm is to evaluate the effect of encounters with high energy particles.

The time history of the spacecraft ground, shaded Teflon cell voltage and solar array voltages for the encounter with this type of substorm is shown in figures 9(a) and (b). In the low density case, the only discharges that occur are in the shaded insulator. It is interesting to note that these discharges did not occur during the 12 keV electron temperature peak but only after the substorm started to decay. The solar array did not discharge throughout the encounter.

In the high density case shaded insulator discharges during the peak intensity encounter. Major discharges involving most of the shaded solar array and spacecraft body insulator surfaces did occur after the substorm intensity started to decay. When the substorm electron temperature fell to the 4 keV level, all discharge activity ceased. The voltage distributions around the satellite were similar to those seen in the category 2 substorm case.

Discussion

The results of this study indicates that the time variations and particle densities in substorms are important in determining whether discharges will occur on spacecraft. An encounter with a very intense substorm that has a very low particle density (~0.1 cm^{-3}) or lasts for a short period of time (<15 min) would not necessarily produce discharges. Conversely, a moderate substorm could cause discharges if the particle densities were high and the substorm duration long.

The observations of the discharges that occurred in the shaded Teflon indicate that the electron temperature has to be about 6 keV for discharges to occur. Furthermore, it appears that there is a consistent relationship between an electron incident energy density and breakdowns. If the electron temperature, E_e, and the electron density, n_e, is converted to an incident electron current density (j_e) by the relationship:

$$j_e = 2.7 \times 10^{-12}\, n_e \sqrt{E_e} \qquad \text{amps/cm}^2$$

and this, in turn, multiplied by the temperature and time (in seconds) to obtain the energy density (ε):

$$\varepsilon = E_e j_e t \qquad \text{joules/cm}^2,$$

then, the incident energy density to obtain the first discharge is about 1.2 mjoules/cm^2 and the subsequent discharges occur when the energy density is about 1 mjoule/cm^2. Major discharges seem to occur when this energy density

is about 2 mjoule/cm^2, but also has an, as yet undetermined, relationship to electron temperature and prior charging history.

It must be stressed that the numbers obtained for incident energy density apply only to this satellite and to the breakdown criteria used (~10^5 V/cm and 67% of charged transferred). If different criteria were used, the number would change, but the concept of relating discharges to incident energy would still hold. This points out the importance of developing a design guideline, time-varying, geomagnetic substorm to be used to determine if future satellite designs would be susceptible to discharges. In addition the design guideline substorm would be useful in developing the absolute discharge criteria.

CONCLUDING REMARKS

The NASCAP computer code has been utilized to study the behavior of a typical geosynchronous, 3-axis stabilized, communications satellite in a variety of idealized geomagnetic substorms. In all cases sunlight was incident on the solar array at a 27° angle to the normal to simulate a June or January orbiting condition. The sun angle caused shadowing of parts of the spacecraft surfaces and is expected to enhance differential charging.

It has been found that charging of satellite surfaces in sunlight is a relatively slow process which can take hours for the insulator surface voltages to reach equilibrium. Since substorms are known to be time-varying in their intensity and particle densities, it is not logical to expect equilibrium surface voltage conditions to exist in a realistic duration substorm. Hence, transient spacecraft charging computations are needed and NASCAP can fill this need. For such transient calculations, it has been found that particle densities (and hence incident current densities) must be well known throughout the substorm since variations of factors of two can make significant differences in the predicted surface voltages.

The model used in this study was compared to the results obtained with the ATS-6. For the same substorm characteristics (5.6 keV electron temperature, 14 keV proton temperature and 0.2 particles/cm^3) the NASCAP model predicted that the ground potential would approach the ATS-6 measured value of -700 volts in about 40 minutes. This was believed to be a reasonable approximation since 3-axis stabilized satellites should attain the same ground potential.

The discharge criteria imposed in this study was that the insulators would breakdown under on edge voltage gradient of 1.5×10^5 volts/cm. Furthermore, it was assumed that when breakdown occurred, the discharge would be simulated by allowing 67% of the surface charge to be transferred to the conductor beneath, distributed and all potentials recalculated. This criteria was applied uniformly to all materials used at the start of computations and allowed to occur automatically.

Substorms were defined in 30 min steps and two number densities were evaluated for each substorm to evaluate rate effects. It was found that there is a minimum electron temperature for discharges to occur. With the materials, configuration and discharge criteria used in this study, this minimum temperature

was found to be 6 keV. It was also found that there is a minimum input energy density required to cause discharges. In this study, it appears that discharges seem to be initiated whenever the electron temperature is larger than the minimum and the input electron energy density exceeds 1.2 mjoules/cm^2. Major discharges involving large numbers of shaded surfaces seem to be possible when the input electron energy density exceeds 2 mjoules/cm^2 but this result can be influenced by prior charging conditions. It is also possible for these conditions to be met after the peak of the substorm so that discharges can occur during a decaying substorm.

The characteristics of the discharges observed in this study are similar to those seen in the laboratory investigations. The charging rate after discharges is more rapid than before and the discharge rate is more dependent on the incident current density than the electron temperature.

The result obtained here must be considered preliminary and the first step in an continuing evaluation of this phenomenon. Discharge characterization must be better defined and the simulation improved. Substorm parameters as function of time must be catalogued along with the spacecraft ground potentials caused by the substorm. This will aid validation of the modelling techniques. Even with these limitations, the present study has indicated trends that were not apparent before and has pointed out areas where additional work is required.

REFERENCES

1. S. E. DeForest and C. E. McIlwain, "Plasma Clouds in the Magnetosphere," J. Geophys. Res., vol. 76, pp. 3587-3611, June 1971.

2. R. C. Olsen, E. C. Whipple, and C. K. Purvis, "Active Modification of ATS-5 and ATS-6 Spacecraft Potentials," in Effect of the Ionosphere on Space and Terrestrial Systems, John M. Goodman, Ed. Washington, D.C.: Naval Research Lab., 1978, pp. 328-336.

3. D. L. Reasoner, W. Lennartsson, and C. R. Chappell, "Relationship Between ATS-6 Spacecraft-Charging Occurrences and Warm Plasma Encounters," in Spacecraft Charging by Magnetospheric Plasmas, A. Rosen, Ed. Progress in Astronautics and Aeronautics, Vol. 47, New York: American Institute of Aeronautics and Astronautics, 1976, p. 89.

4. S. E. DeForest, "Spacecraft Charging at Synchronous Orbits," J. Geophys. Res., vol. 77, pp. 651-659, February 1972.

5. A. Rosen, "Spacecraft Charging-Environment Induced Anomalies," AIAA Paper 75-91, Jan. 1975.

6. R. R. Lovell, N. J. Stevens, W. Schober, C. P. Pike, and W. L. Lehn, "Spacecraft Charging Investigation: A Joint Research and Technology Program," in Spacecraft Charging by Magnetospheric Plasmas, A. Rosen, Ed. Progress in Astronautics and Aeronautics, Vol. 47, New York: American Institute of Aeronautics and Astronautics, 1976, p. 3.

7. J. C. Durrett, and J. R. Stevens, "Description of the Space Test Program P78-2 Spacecraft and Payloads," in Spacecraft Charging Technology - 1978. NASA CP-2071 and AFGL TR-79-0082, 1979, pp. 4-10.

8. G. T. Inouye, "Spacecraft Charging Model," AIAA Paper 75-255, Jan. 1975.

9. M. J. Massaro, and D. Ling, "Spacecraft Charging Results for the DSCS-III Satellite," in Spacecraft Charging Technology - 1978. NASA CP-2071 and AFGL TR-79-0082, 1979, pp. 158-178.

10. C. K. Purvis, "Effects of Secondary Electron Yield Parameter Variations on Predicted Equilibrium Potentials of an Object in a Charging Environment," Presented at the 1979 IEEE Annual Conference on Nuclear and Space Radiation Effects, Paper G-1, July 1979.

11. I. Katz, J. J. Cassidy, M. J. Mandell, G. W. Schnuelle, P. G. Steen, and J. C. Roche, "The Capabilities of the NASA Charging Analyzer Program," in Spacecraft Charging Technology - 1978. NASA CP-2071 and AFGL TR-79-0082, 1979, pp. 101-122.

12. I. Katz, D. E. Parks, M. J. Mandell, J. M. Harvey, D. H. Brownell, Jr., S. S. Wang, and M. Rotenberg, "A Three-Dimensional Dynamic Study of Electrostatic Charging in Materials," Systems Science and Software, La Jolla, Calif., rep. SSS-R-77-3367, 1977. (NASA CR-135256)

13. I. Katz, J. J. Cassidy, M. J. Mandell, G. W. Schnuelle, P. G. Steen, D. E. Parks, M. Rotenberg, and J. H. Alexander, "Extension, Validation, and Application of the NASCAP Code," NASA CR-159595, 1979.

14. H. B. Garrett, "Modeling of the Geosynchronous Environment," in Spacecraft Charging Technology - 1978. NASA CP-2071 and AFGL TR-79-0082, 1979, pp. 11-22.

15. P. R. Aron and J. V. Staskus, "Area Scaling Investigations of Charging Phenomena," in Spacecraft Charging Technology - 1978. NASA CP-2071 and AFGL TR-79-0082, 1979, pp. 485-506.

16. K. G. Balmain, "Scaling Laws and Edge Effects for Polymer Surface Discharges," in Spacecraft Charging Technology - 1978. NASA CP-2071 and AFGL TR-79-0082, 1979, pp. 646-656.

17. E. J. Yadlowsky, R. C. Hazelton, and R. J. Churchill, "Characterization of Electrical Discharges on Teflon Dielectrics Used as Spacecraft Thermal Control Surfaces," in Spacecraft Charging Technology - 1978. NASA CP-2071 and AFGL TR-79-0082, 1979, pp. 632-645.

18. N. J. Stevens, C. K. Purvis, and J. V. Staskus, "Insulator Edge Voltage Gradient Effects in Spacecraft Charging Phenomena," IEEE Trans. Nucl. Sci., vol. NS-25, pp. 1304-1312, December 1978.

19. N. J. Stevens, F. D. Berkopee, J. V. Staskus, R. A. Blech, and S. J. Narcisco, "Testing of Typical Spacecraft Materials in a Simulated Substorm Environment," in Proceedings of the Spacecraft Charging Technology Conference, C. P. Pike and R. R. Lovell, Eds. NASA TM X-73537/AFGL TR-77-0051, 1977 pp. 431-457.

20. M. J. Mandell, I. Katz, G. W. Schnuelle, P. G. Steen, and J. C. Roche, "The Decrease in Effective Photocurrents Due to Saddle Points in Electrostatic Potentials Near Differently Charged Spacecraft," in IEEE Trans. Nucl. Sci., vol. NS-25, pp. 1313-1317, December 1978.

21. N. J. Stevens, and R. R. Lovell, "Spacecraft Charging Investigation for the CTS Project," in Spacecraft Charging by Magnetospheric Plasmas, A. Rosen, Ed. Progress in Astronautics and Aeronautics, vol. 47, New York: American Institute of Aeronautics and Astronautics, pp. 263-275, 1976.

22. C. K. Purvis, J. V. Staskus, J. C. Roche, and F. D. Berkopec, "Charging Rates of Metal-Dielectric Structures," in Spacecraft Charging Technology - 1978. NASA CP-2071 and AFGL TR-79-0082, 1979, pp. 507-523.

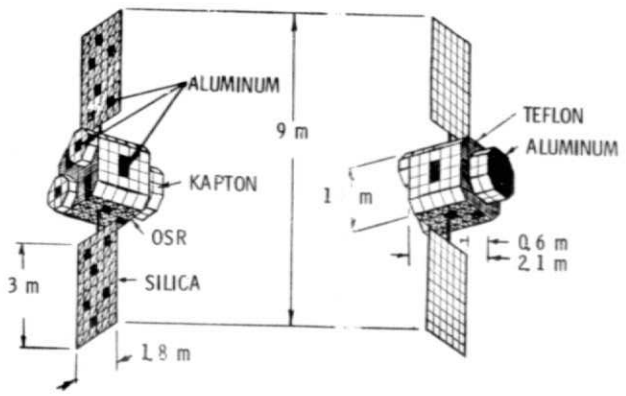

Figure 1. - Typical geosynchronous communications satellite.

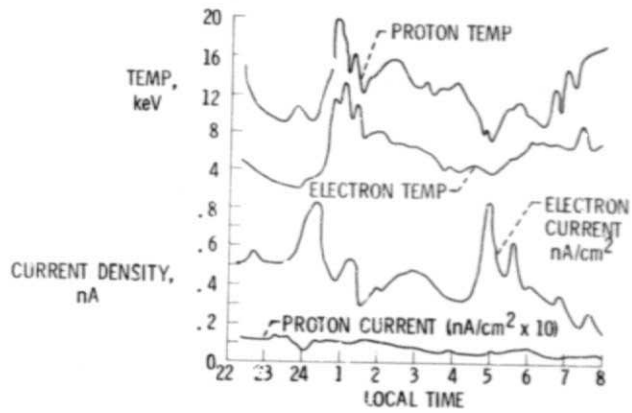

Figure 2. - Environmental conditions from January 2, 1970 substorm.

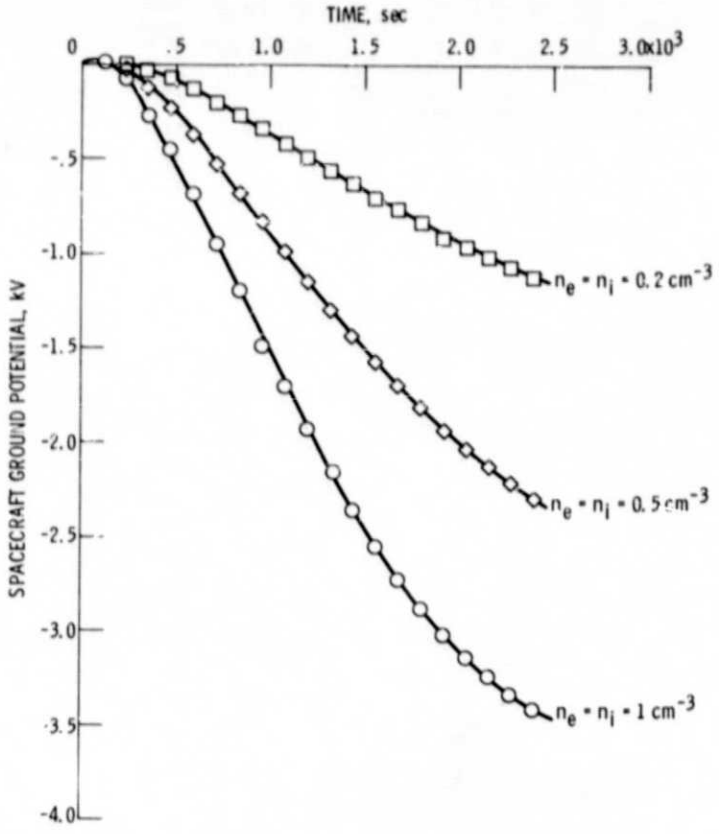

Figure 3. - Variation of spacecraft ground potential with substorm plasma density; T_e = 8 keV, T_i = 14 keV.

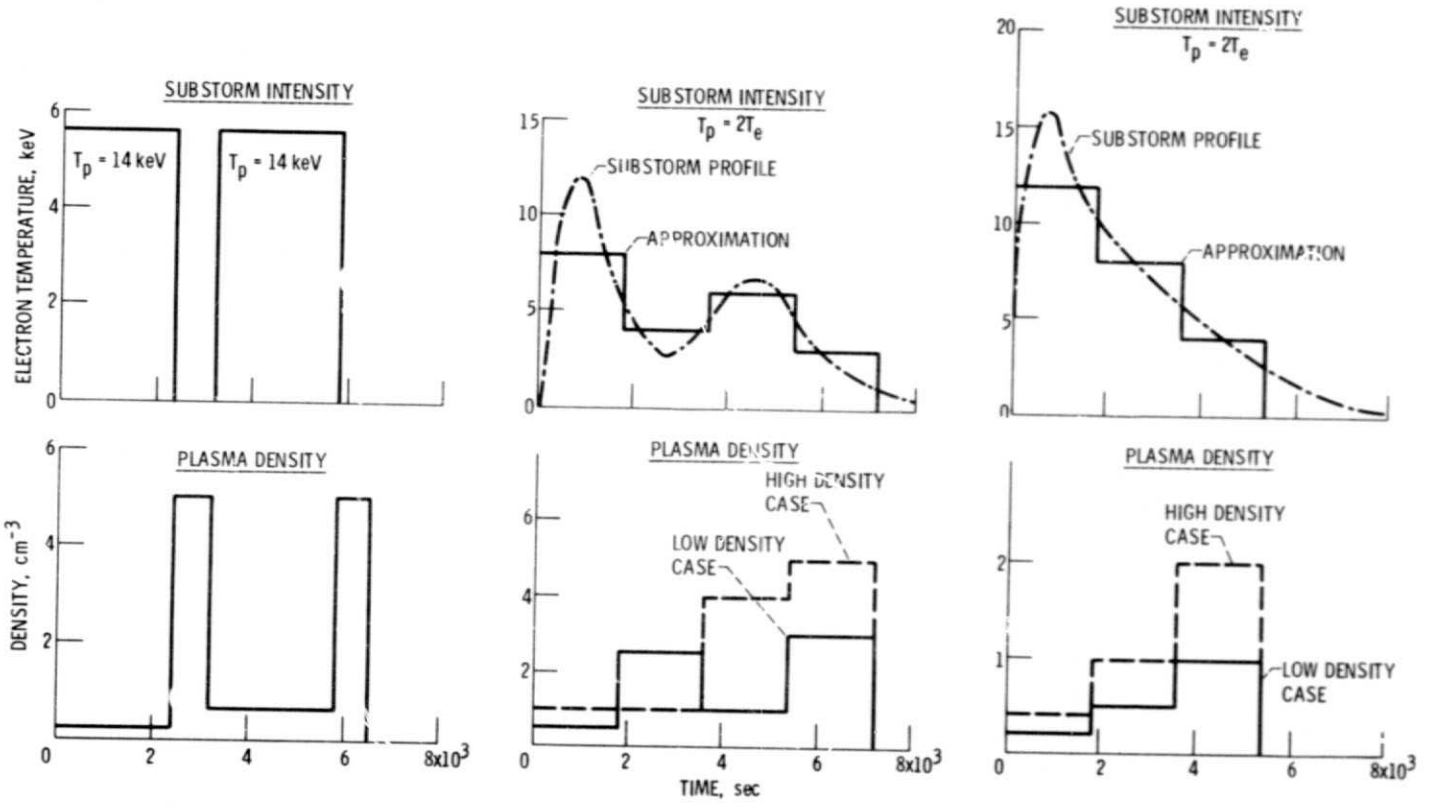

(a) CATEGORY 1 SUBSTORM.

(b) CATEGORY 2 SUBSTORM.

(c) CATEGORY 3 SUBSTORM.

Figure 4. - Summary of substorm environments.

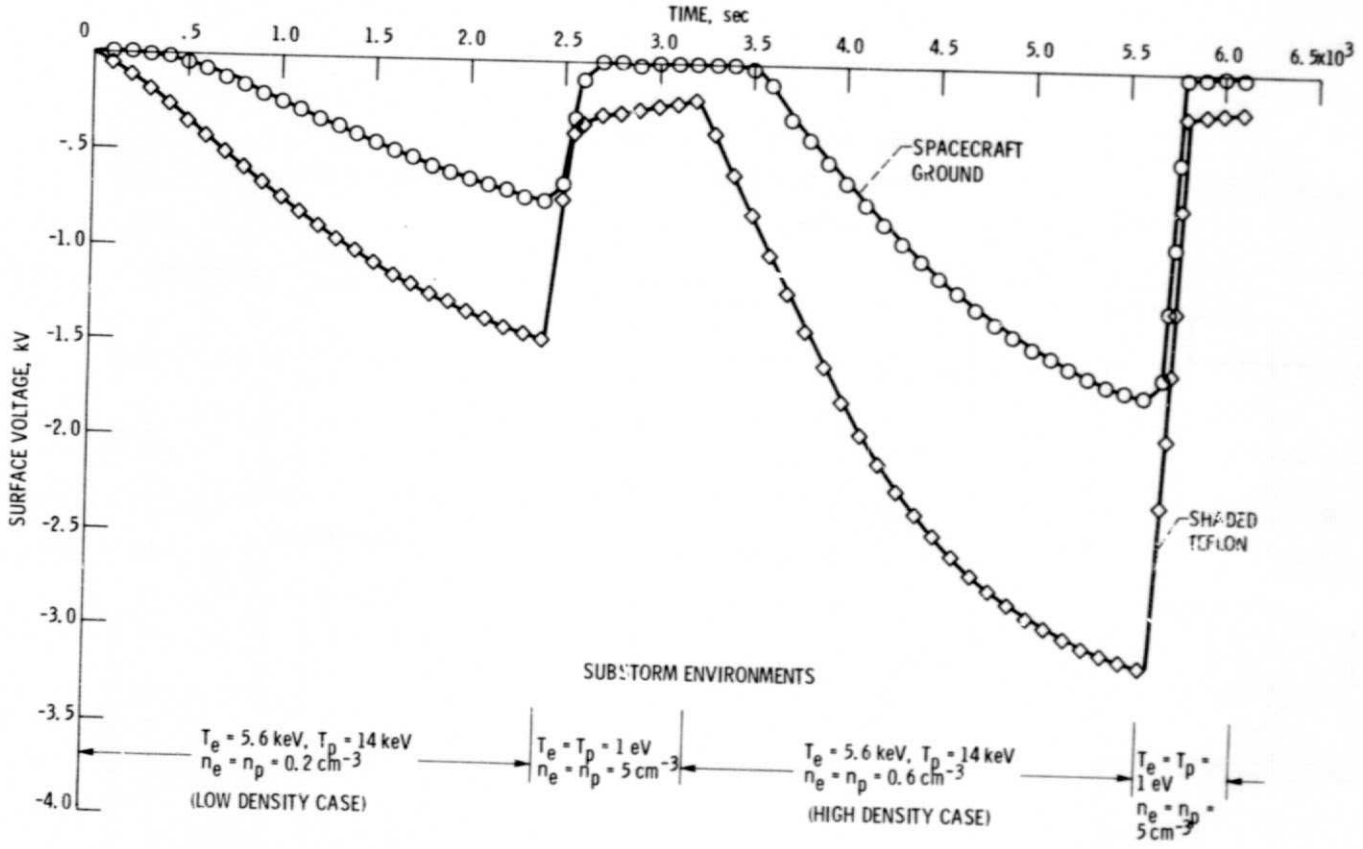

(a) SPACECRAFT BODY RESPONSE.

Figure 5. - Satellite response to category 1 substorm environment.

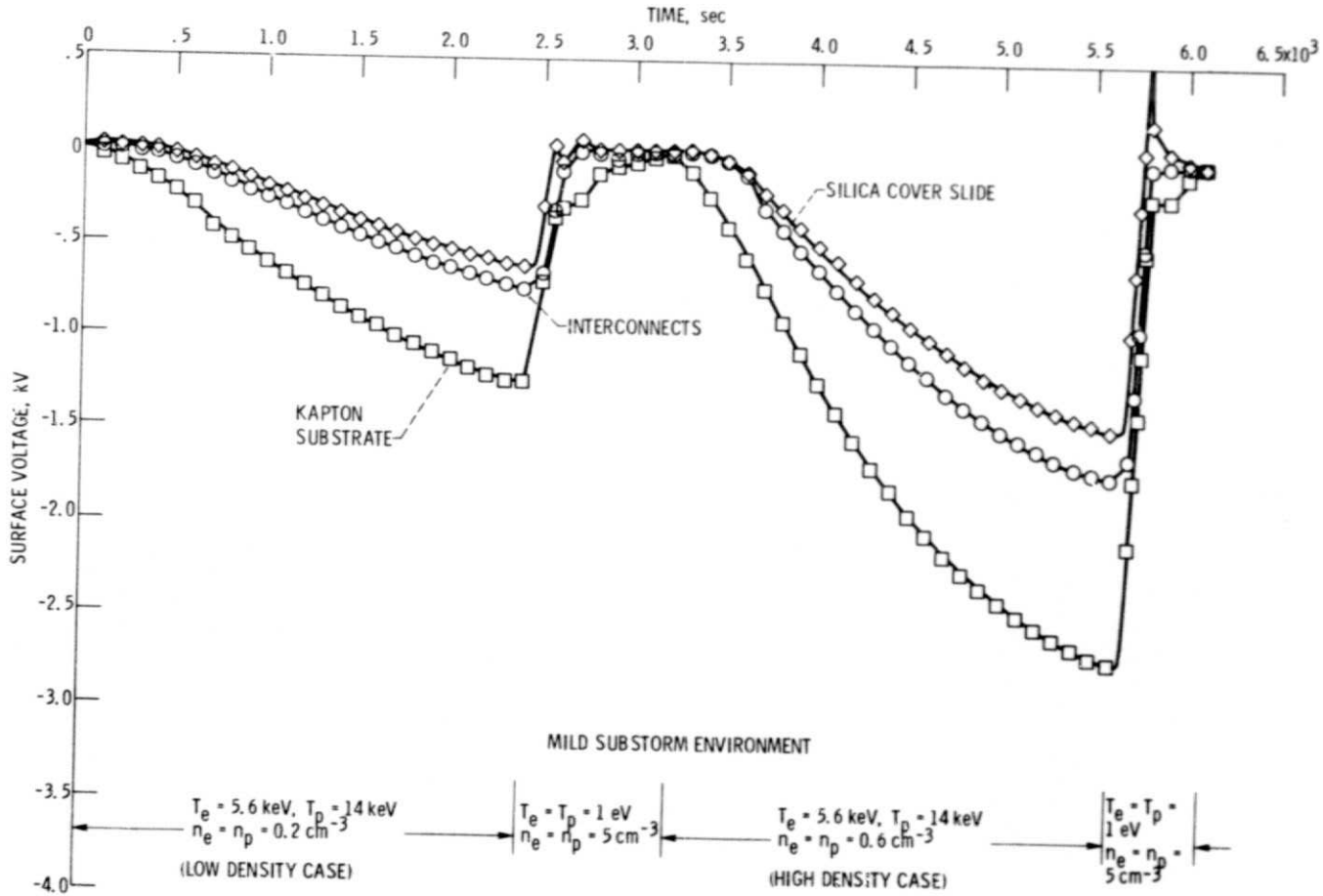

(b) SOLAR ARRAY RESPONSE.

Figure 5. - Concluded.

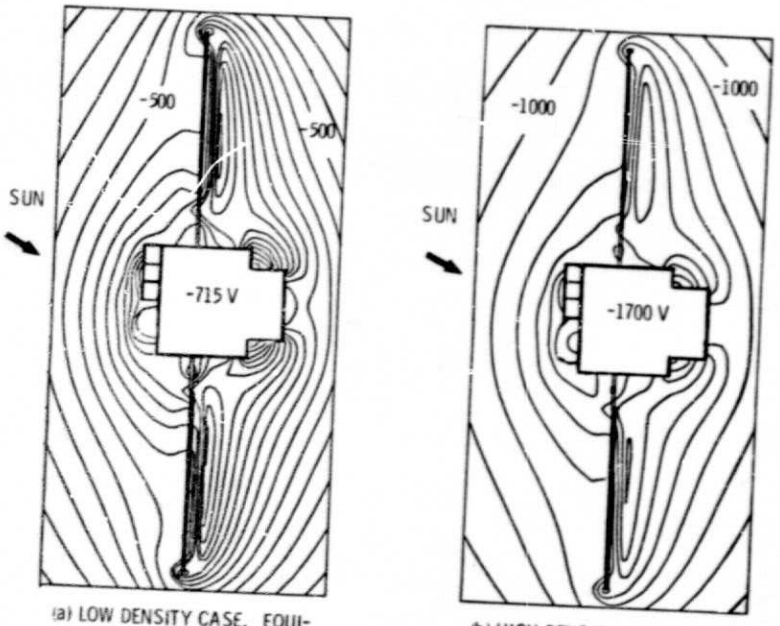

(a) LOW DENSITY CASE. EQUI-POTENTIAL LINES IN 50 V STEPS.

(b) HIGH DENSITY CASE. EQUI-POTENTIAL LINES IN 200 V STEPS.

Figure 6. - Voltage profiles around satellite. Category 1 substorm.

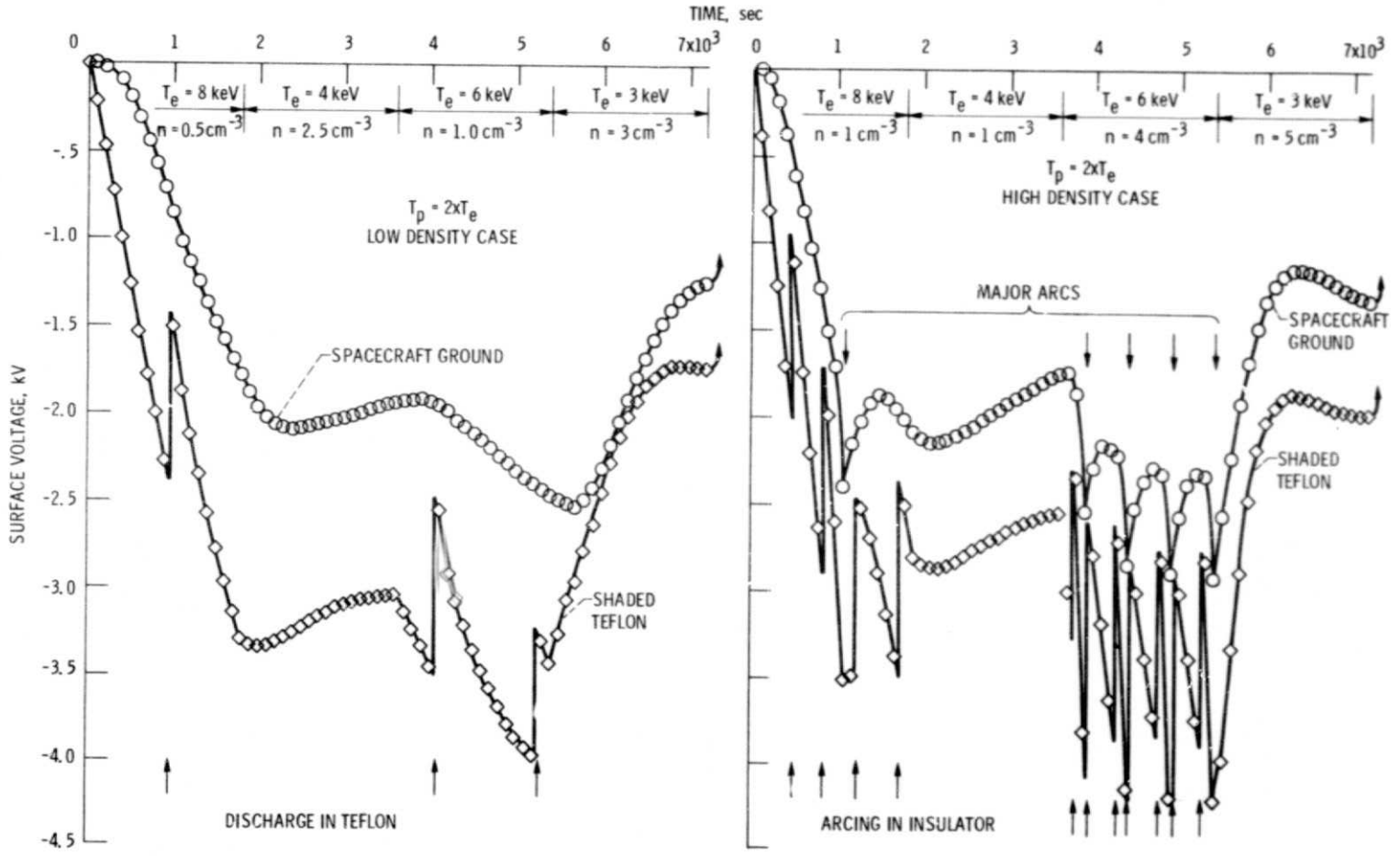

(a) SPACECRAFT BODY RESPONSE.

Figure 7. - Satellite response to category 2 substorm environment.

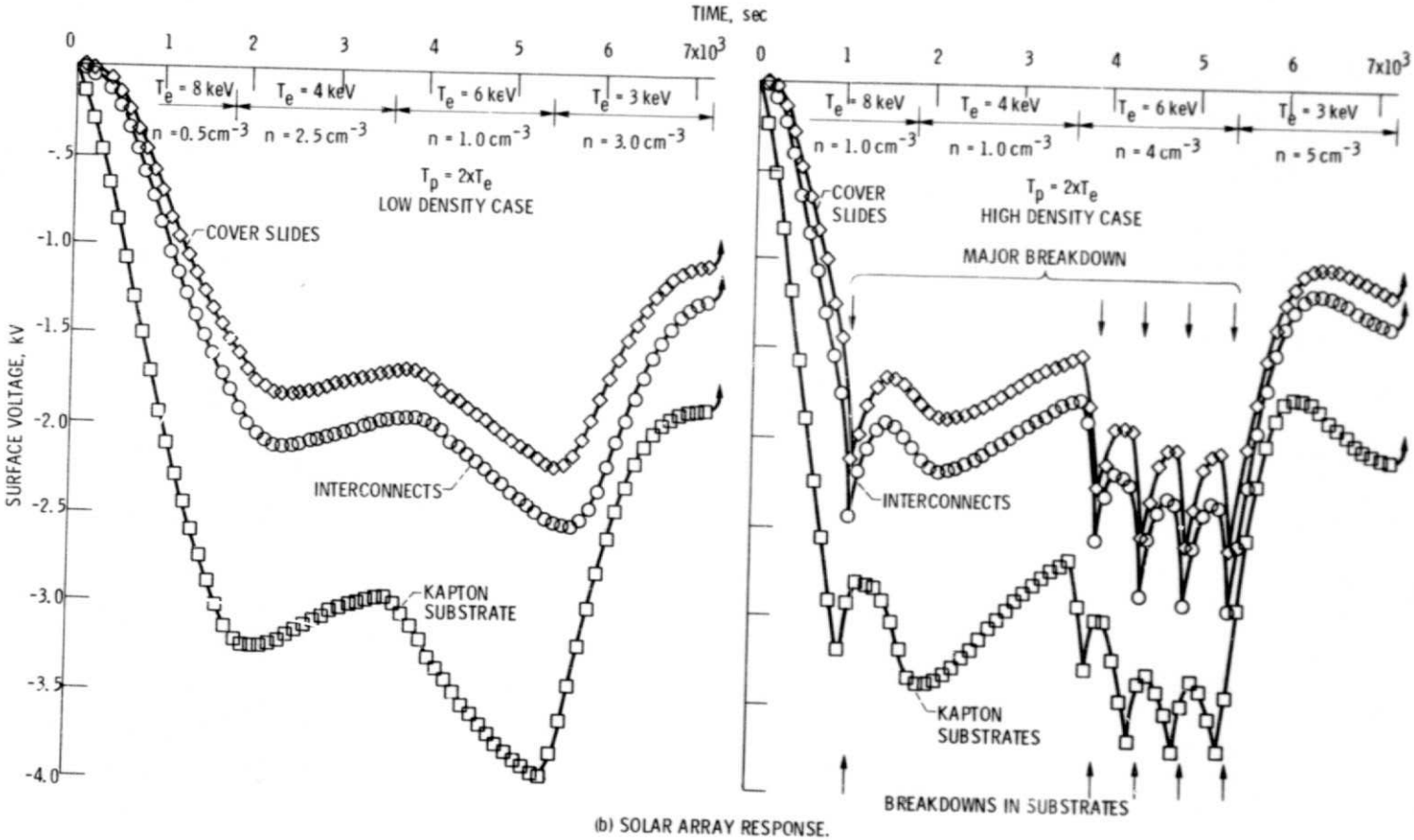

(b) SOLAR ARRAY RESPONSE.

Figure 7. - Concluded.

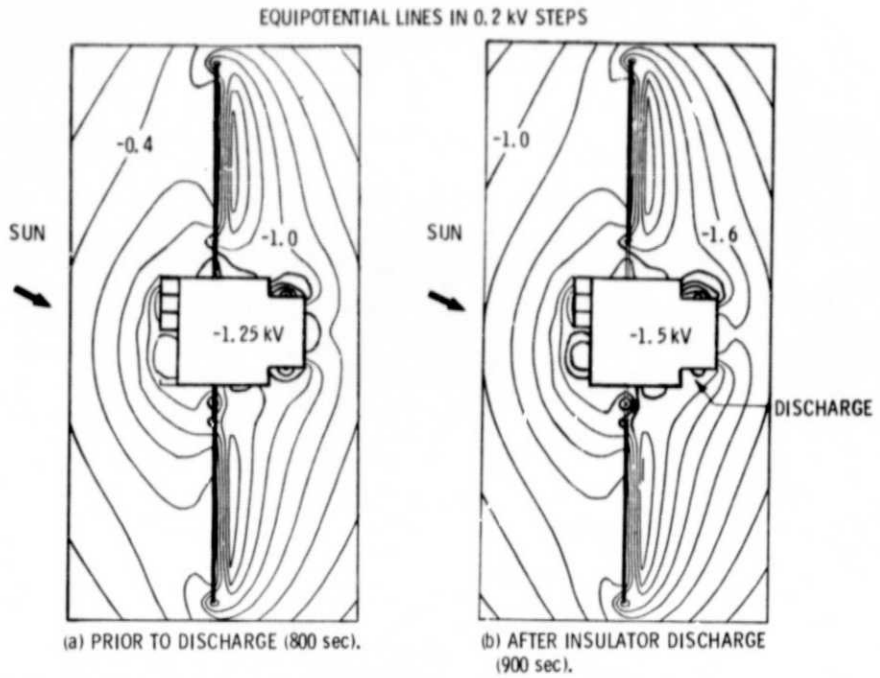

(a) PRIOR TO DISCHARGE (800 sec).

(b) AFTER INSULATOR DISCHARGE (900 sec).

Figure 8. - Voltage profiles around satellite during discharges. Category 2 substorm.

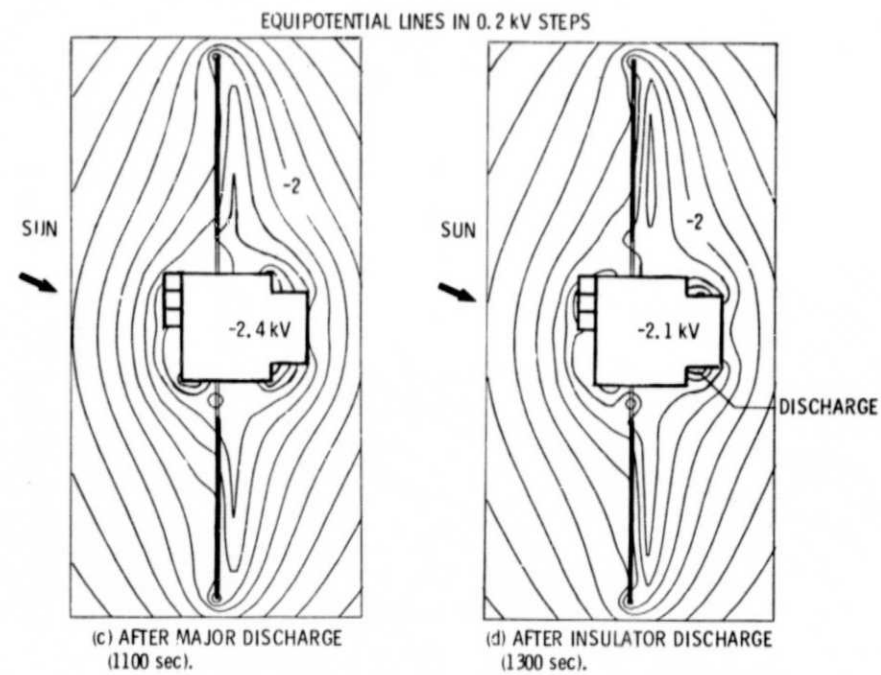

(c) AFTER MAJOR DISCHARGE (1100 sec).

(d) AFTER INSULATOR DISCHARGE (1300 sec).

Figure 8. - Concluded.

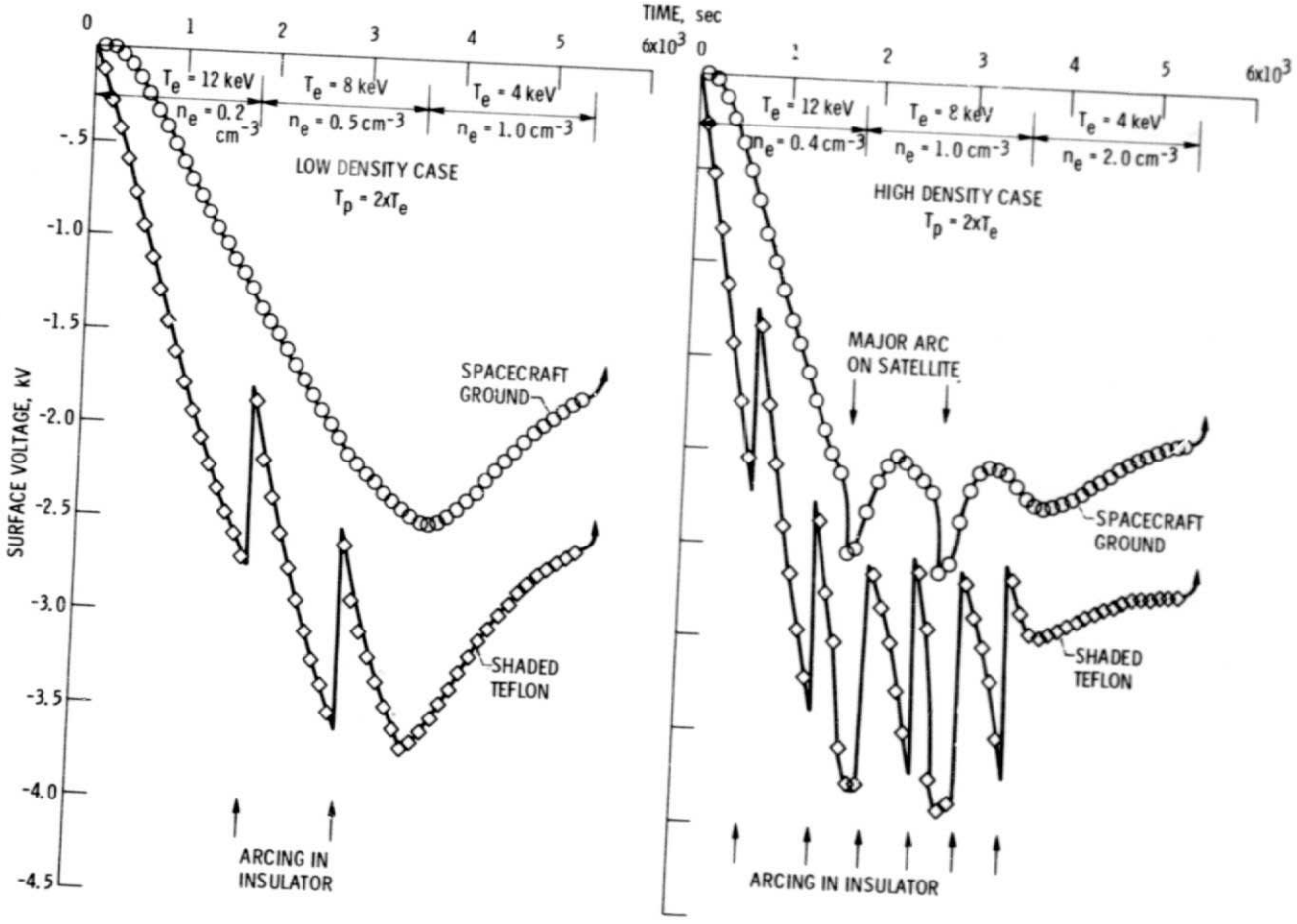

(a) SPACECRAFT BODY RESPONSE.

Figure 9. - Satellite response to category 3 substorm environment.

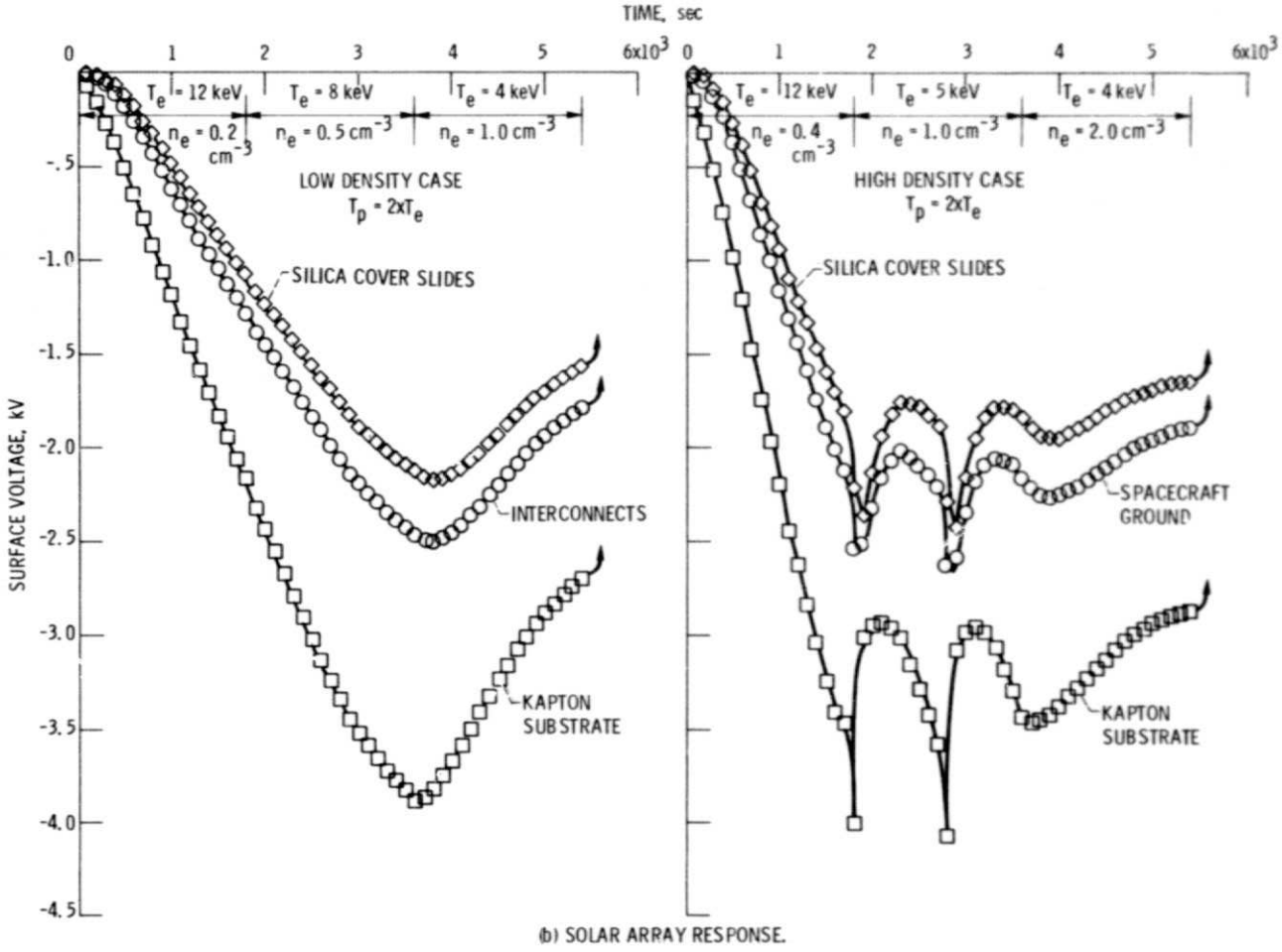

(b) SOLAR ARRAY RESPONSE.

Figure 9. - Concluded.